Journal of Human Genetics (2019) 64:1203–1217
https://doi.org/10.1038/s10038-019-0653-x

ARTICLE

MicroRNA-370 functions as a tumor suppressor in hepatocellular carcinoma via inhibition of the MAPK/JNK signaling pathway by targeting BEX2

Xin Wang[1] · Wenyan Zhu[2] · Chuanshen Xu[3] · Feng Wang[1] · Xiaodan Zhu[1] · Yandong Sun[1] · Yuan Guo[4] · Xiaoyue Fu[1] · Yong Zhang[1] · Yunjin Zang[1]

Received: 11 January 2019 / Revised: 8 July 2019 / Accepted: 23 July 2019 / Published online: 17 September 2019

Abstract

Hepatocellular carcinoma (HCC) is a primary malignancy of the liver and occurs predominantly in patients with underlying chronic liver disease and cirrhosis. Accumulating studies have revealed that microRNAs (miRNAs) play a critical role in the development and progression of HCC. Through microarray-based gene expression profiling of HCC, miR-370, and BEX2 were identified in HCC. Hence, this study aimed to evaluate their abilities on the cellular processes in HCC. It was determined that BEX2 was highly expressed and miR-370 was poorly expressed in HCC cell lines and tissues. Then, the cell line presenting with the highest BEX2 expression and the lowest miR-370 expression was selected for subsequent gain- and loss-of-function experimentation. The antitumor effect of miR-370 on HCC cell proliferation, invasion, migration, and apoptosis, as well as the MAPK/JNK signaling pathway was examined. Meanwhile, the interaction among miR-370, BEX2, and MAPK/JNK signaling pathway was identified. BEX2 is verified to be a target of miR-370. Moreover, miR-370 exerted antitumor effect on HCC development through suppression of the MAPK/JNK signaling pathway by targeting BEX2. Later, it was further verified by in vivo experiment that overexpression of miR-370 inhibited tumor growth. Above results provide evidence that miR-370 could downregulate BEX2 gene and inhibit activation of MAPK/JNK signaling pathway, thus inhibiting the development of HCC. It provides a worth-trying novel therapeutic target for HCC treatment.

Introduction

Hepatocellular carcinoma (HCC) is a solid life-threatening malignant tumor ranking as the 3rd leading cause of tumor-related deaths around the world [1]. For patients with HCC, metastasis and recurrence are the primary factors resulting in poor prognoses of HCC patients [2]. The high mortality rates of HCC can be attributed to a lack of early diagnosis and the ensuing poor prognosis related with high metastasis and recurrence rate of patients diagnosed at advanced stages after nonradical treatment [3]. Furthermore, microRNAs (miRNAs) have been reported to participate in several kinds of cell biological processes, including cell proliferation, differentiation, motility, apoptosis, angiogenesis, and metastasis [4]. More intriguingly, a number of miRNAs have been identified to be capable of alleviating HCC progression by downregulating genes, which work to inhibit tumor suppressor and enhance the expression of oncogenes [5].

miRNAs serve as both a promoter and suppressor of tumor growth in numerous types of cancers [6]. Moreover, various miRNAs have been implicated in the pathogenesis of cancers, making miRNA involvement an important biology for cancers [7]. As one of the endogenous non-coding RNAs, miR-370 plays a vital role in carcinogenesis, and specifically, miR-370 was found to suppress tumor development by targeting the forkhead box protein [8]. Brain-expressed X-linked 2 (BEX2) is a member of the

These authors contributed equally: Xin Wang, Wenyan Zhu

✉ Yunjin Zang
zangyj3657@qq.com

[1] Department of Liver Transplantation, The Affiliated Hospital of Qingdao University, 266000 Qingdao, PR China

[2] Operating Room, The Affiliated Hospital of Qingdao University, 266000 Qingdao, PR China

[3] Transplantation Care Unit, The Affiliated Hospital of Qingdao University, 266000 Qingdao, PR China

[4] Department of Liver Surgery, The Affiliated Hospital of Qingdao University, 266000 Qingdao, PR China

BEX family, which functions to regulate the development of nervous system, as well as the process of cancer [9]. It was reported that downregulation of BEX2 was involved in the inhibition of cell proliferation and promotion of cell apoptosis in malignant glioma by regulating the c-Jun NH2 terminal kinase (JNK) signaling pathway [10]. JNK is an evolutionarily conserved mitogen-activated protein kinase (MARK) that regulates cell survival, proliferation, and cell death [11]. In tumorigenesis, the JNK signaling pathway is frequently dysregulated and is effective in regulating tumor cell proliferation [12], and thus may also play a role in HCC treatment. On the basis of aforementioned evidence, it can be subsequently concluded that miR-370 might participate in the regulation of tumor progression in HCC by modulating the expression of BEX2 and the MARK/JNK signaling pathway-related genes, so as to provide a novel therapeutic target for the treatment of HCC.

Materials and methods

Microarray-based gene expression profiling

Two HCC expression datasets (GSE62232 and GSE45267) were retrieved from the Gene Expression Omnibus (GEO) database (https://www.ncbi.nlm.nih.gov/geo/), among which the GSE45267 dataset included both elderly and young samples. The two groups of samples were comprised of normal controls and HCC samples. Subsequently, differential analysis was conducted for the elderly and young samples. The R language "limma" package was applied to analyze the differentially expressed genes with $|\log FC| > 2$ and p value < 0.05 serving as the screening criteria. The heat map of differentially expressed genes was plotted using the "heat map" package. The Venn diagram was plotted on the website (http://bioinformatics.psb.ugent.be/webtools/Venn/) so as to obtain the intersection of the differentially expressed genes.

In addition, the MalaCards database (http://www.malacards.org/) was employed to search for known genes of HCC. Furthermore, the STRING database (https://string-db.org/) was utilized to analyze possible relation between the known genes and the differentially expressed genes, and a gene–gene interaction network map was constructed.

GEPIA (http://gepia.cancer-pku.cn/detail.php), a newly developed interactive web, serves for analyzing RNA sequencing expression data of 9736 tumors and 8587 normal samples from the TCGA and the GTEx projects through a standard processing pipeline. The BEX2 expression was further verified in this database. The DIANA database (http://diana.imis.athena-innovation.gr/DianaTools/index.php?r=microT_CDS/index), miRDB database (http://mirdb.org/miRDB/index.html), mirDIP database (http://ophid.utoronto.ca/mirDIP/index.jsp#r), and the miRNA searching database (https://www.exiqon.com/miRSearch) were also employed to predict the miRNAs, which regulate BEX2. A Venn diagram was drawn to obtain the intersection of the predicting results in the aforementioned four databases.

Study subjects

From July 2013 to July 2016, a total of 76 HCC tissues and adjacent normal tissues were collected from patients (with a mean age of 54.25 years) who underwent resection of HCC malignant tumor at the Affiliated Hospital of Qingdao University. Pathological confirmation was carried out to verify that all enrolled cases were HCC patients, and no patients underwent chemoradiotherapy prior to the operation. Among all subjects, there were 40 cases aged ≥55 years old, 36 cases <55 years old, including 42 males and 34 females. There were 44 cases with liver cirrhosis; 17 cases whose tumor diameter <5 cm, and 59 cases whose tumor diameter ≥5 cm. A total of 37 cases presented with vascular invasion and 39 cases with no vascular invasion. The tumor node metastasis (TNM) stage of HCC tumor: stage I and II, $n = 48$; stage III and IV, $n = 28$. In addition, there were 40 cases with capsular invasion and 36 cases without capsular invasion [13]. All HCC tissues and adjacent normal tissues were stored in a frozen pipe with liquid nitrogen, which were later stored at −80 °C.

Reverse transcription quantitative polymerase chain reaction (RT-qPCR)

Total RNA content of HCC and adjacent normal tissues were extracted according to the instructions of Trizol Kit (5003050, Shanghai Mingjing Biotechnology Co., Ltd, Shanghai, China). After performing reverse transcription using an ABI7500 quantitative PCR instrument (ABI7500, Zhiyan Scientific Instruments Co., Ltd, Shanghai, China), real-time PCR assay was further applied to detect the expression patterns of miR-370, BEX2, JNK, extracellular-signal-regulated kinases (ERK), c-Jun, and c-Fos. U6 was regarded as the internal reference for miR-370, and glyceraldehyde-3-phosphate dehydrogenase (GAPDH) was considered as the internal reference for the other genes. The primer sequences are shown in Table 1. Relative expression of the detected genes was calculated using the $2^{-\triangle\triangle Ct}$ method. Each set of experiments was repeated three times, and the above experiment was also suitable for cell experiments.

Western blot analysis

HCC tissues were lysed using 1 mL tissue lysis buffer (EHJSW-109124, Huijia Biotechnology Co., Ltd,

Table 1 Primer sequences for reverse transcription quantitative polymerase chain reaction

Gene	Primer sequences
miR-370	Upstream: 5′-GCCTGCTGGGGTGGAACCTGGTAA-3′
	Downstream: 5′-GCGAGCACAGAATTAATACGAC-3′
U6	Upstream: 5′-CTCGCTTCGGCAGCACA-3′
	Downstream: 5′-AACGCTTCACGAATTTGCGT-3′
BEX2	Upstream: 5′-AAAGAGGAACGAGCGTTAAACA-3′
	Downstream: 5′-TCACTAACATTCAAAGGTAGGGC-3′
JNK	Upstream: 5′-TGAGAAACTCTTCCCTGATG-3′
	Downstream: 5′-GCTTCAGAAGGATCATACCA-3′
ERK	Upstream: 5′-GGAAGCATTATCTTGACCAG-3′
	Downstream: 5′-CTCTTGTGTGCGTTGAATGT-3′
c-Jun	Upstream: 5′-ATGACTGCAAAGATGGAAACGACC-3′
	Downstream: 5′-TGTTTGCAACTGCTGCGTTAGCATG-3′
c-Fos	Upstream: 5′-CCTGTACTCCCAGCTGCACTGCTTA-3′
	Downstream: 5′-TCACAGGGCCAGCAGCGTGGGTGAG-3′
GAPDH	Upstream: 5′-GGAGCGAGATCCCTCCAAAAT-3′
	Downstream: 5′-GGCTGTTGTCATACTTCTCATGG-3′

miR-370 microRNA-370, *BEX*2 brain-expressed X-linked protein 2, *JNK* c-Jun NH2 terminal kinase, *ERK* extracellular-signal-regulated kinases, *GAPDH* glyceraldehyde-3-phosphate dehydrogenase

Xiamen, China). Then, the protein concentration was determined using a bicinchoninic acid kit (JK-201, Shanghai JingkeScience and Technology Co., Ltd, Shanghai, China), followed by electrophoresis separation using 10% sodium dodecyl sulfate (SDS) separation gel and concentration gel. Later, the proteins were transferred onto a nitrocellulose membrane, which was then blocked by 5% skimmed milk powder overnight at 4 °C. The following day, the membrane was further incubated with the following primary rabbit polyclonal antibodies: BEX2 (ab213424, dilution ratio of 1:1000), ERK (ab184699, dilution ratio of 1:10000), JNK (ab112501, dilution ratio of 1:1000), c-Jun (ab31419, dilution ratio of 1:1000), c-Fos (ab190289, dilution ratio of 1: 2000), p-ERK (ab214362, dilution ratio of 1:1000), p-JNK (ab4821, dilution ratio of 1:1000), p-c-Jun (ab32385, dilution ratio of 1:1000), and GAPDH (ab181602, dilution ratio of 1:10000) overnight. Subsequently, the membrane was incubated for 1 h with horseradish peroxidase (HRP)-labeled immunoglobulin G (IgG) goat anti-rabbit secondary antibody (ab109489, dilution ratio of 1:1000). All aforementioned antibodies were purchased from Abcam Inc., Cambridge, MA, USA. After that, the membrane was reacted with enhanced chemiluminescence (ECL) solution (ECL808–25, Biomiga, San Diego, CA, USA) for 1 min to observe the results. The ratio of the gray value of the target band to GAPDH was representative of the relative protein expression. Each experiment was repeated three times to obtain the mean value. The above experimental procedures were also suitable for cell experiments.

Cell culture

HCC cell lines Hep3B, SK-hep-1, YY8103, MHCC-97H, C3A, and HepG2 (Shanghai North Connaught Biotechnology Co., Ltd, Shanghai, China) were cultured in a Roswell Park Memorial Institute 1640 medium containing 10% fetal bovine serum in a humidified incubator (IL-161CT, Chengdu Yuqiang Technology Co., Ltd, Sichuan, China) with 5% CO_2 in air at 37 °C. The culture medium was renewed every 24 h and cell passage was performed every 72 h. The mRNA expressions of BEX2 in the six cell lines were detected by RT-qPCR, and the cell line with the highest BEX2 expression and lowest miR-370 expression was selected for subsequent experimentation. The above procedures were repeated three times to obtain the mean value.

Dual luciferase reporter gene assay

Analysis of target gene of miR-370 was performed using the biological prediction site, www.microRNA.org, and a dual luciferase reporter gene assay was applied to verify whether BEX2 was the direct target gene of miR-370. A gene fragment containing binding sites was introduced into the pEIR-reporter using the SpeI and HindIII endonuclease sites. Mutant (Mut) sites on the complementary sequence of the seed sequence were synthesized on the wide-type (Wt) BEX2. After being detached with restriction enzyme, T4 DNA ligase was used to insert the target fragments into the pMIR-reporter reporter plasmids. The correctly sequenced luciferase reporter plasmids Wt and Mut were co-transfected with miR-370 mimic into the Hep3B cells (C01-AW, Shanghai North Connaught Biotechnology Co., Ltd, Shanghai, China). After 48-h transfection, the cells were collected and lysed, centrifuged for 3–5 min, and the supernatant was obtained. A luciferase assay kit (T003, Vigorous Biotechnology Beijing Co., Ltd, Beijing, China) was employed for detection according to the manual of the dual luciferase reporter gene detection kit. A luminescence detector (Biolum, Xi'an Tianlong Science and Technology Co., Ltd, China) was applied to determine the luminescence signal intensity in the cells. Each experiment was repeated three times to obtain the mean value.

Cell grouping and transfection

Cells were grouped into the following groups: blank (without any transfection), negative control (NC) (transfected with corresponding NC plasmids), miR-370 mimic, miR-370 inhibitor, siRNA-BEX2, and miR-370 inhibitor + siRNA-BEX2 groups after transfection. All the primer sequences were purchased from Shanghai GenePharma Co., Ltd, (Shanghai, China). The cells were seeded into a six-well plate 24 h prior to transfection. When the cell confluence reached around 50%, the cells were transiently

transfected with human HCC cell line with the mediation of lipofectamine 2000 (Invitrogen, USA). The culture medium was refreshed every 6 h, and cells were collected for subsequent experiments 48 h after transfection.

3-(4,5-dimethylthiazol-2-yl)-2,5-diphenyltetrazolium bromide (MTT) assay

When cell growth density in each group reached a certain concentration after transfection, the cells were trypsinized with 0.25% trypsin and made into a single cell suspension. After the cell concentration was adjusted to 2×10^7 cells/mL, the cells were seeded in a 96-well plate (density of 100 μL/well) and incubated in a 37 °C, 5% CO_2 incubator. The culture plates were removed at the 24, 48, 72, and 96 h time intervals, respectively. Then the cells in each well of the plate were incubated with 10 μL MTT solution (GL0247, Beijing Biolab Technology Co., Ltd, Beijing, China) for 4 h avoiding exposure to light, and the culture medium in the 96-well plate was carefully aspirated. Then, the cells in each well were added with 100 μL dimethyl sulfoxide (DMSO) in dark conditions, which were gently shaken and mixed for 10 min. The optical density (OD) value of each well was measured at 570 nm wavelength using a microplate reader (SP-Max 3500FL, Shanghai flash spectrum biological technology Co., Ltd, Shanghai, China). Each experiment was repeated three times to obtain the mean value, and a cell viability curve was drawn with time point as abscissa and OD value as ordinate.

Flow cytometry

After 48-h transfection, HCC cells in each group were collected and centrifuged (178 × *g*, 5 min), and then the supernatant was discarded. Next, the cells were suspended with 2 mL phosphate buffered saline (PBS), and centrifuged at 1610 × *g* for 5 min, with the supernatant removed. Then, 1 mL 75% cold ethanol was used to fix the cells overnight at 4 °C. Then, the cells were stained using propidium iodide (PI)/RNase staining buffer in dark conditions for 60 min. A flow cytometer (DxFLEX, Beckman Coulter Commercial Enterprise Co., Ltd, Shanghai, China) was used to detect the cell cycle. The experiment was repeated three times to obtain the mean value.

The cells were trypsinized, neutralized by adding culture medium, and triturated gently into a cell suspension. The cells were collected in a 15 mL centrifuge tube. After centrifugation, cell apoptosis in each group was detected under the instructions of a cell apoptosis detection kit (KLJC0066, Shanghai Kanglang Biological Technology Co., Ltd, China). The cells were resuspended again in 500 μL binding buffer, added with 5 μL annexin-V and 5 μL PI, gently triturated, mixed, incubated for 15 in dark conditions, and later observed on the flow cytometer for cell apoptosis detection.

Transwell assay

Matrigel was diluted at 1:7 ratio with serum-free culture medium, and the Matrigel-coated wells were placed in an incubator at 37 °C for 4 h before use. After 48-h transfection, the cells were treated with trypsin to make a single cell suspension, followed by resuspension with serum-free culture medium. The cell concentration was adjusted to 3×10^5 cells/mL. After that, 100 μL suspension was obtained and slowly dropped into the Matrigel-coated apical chamber; 600 μL 10% medium with serum was added to the basolateral chamber, and the whole chamber was incubated with 5% CO_2, at 37 °C for 24 h. After incubation, the cells in the apical chamber were wiped, and then, the chamber was fixed in 95% ethanol for 15 min and stained with 0.1% crystal violet for 10 min. At last, the chamber was inverted on a slide and five views were selected randomly for cell number counting and photography under an inverted microscope. The experiment was repeated three times to obtain the mean value.

Scratch test

After transfection for 48 h, the cells in each group were collected and a 200 μL pipette gun was used to draw a vertical line along the center of the culture plate. The scratch lines were observed and photographed under a microscope. After further incubation for 24 h, the scratches in each plate were observed again under a microscope and photographed. The width of each scratch was measured to calculate the healing rate of the scratch = (width of scratch at 0 h − width of scratch at 24 h)/width of scratch at 0 h × 100%. The experiment was repeated three times to obtain the mean value and compare the migration ability of cells in each group.

Xenograft tumor model in nude mice

Thirty BALB/c nude mice (aged 4–6 weeks, weighing 16–20 g) (purchased from the Laboratory Animal Center of Sun Yat-sen University) were randomly divided into the blank, NC, miR-370 mimic, miR-370 inhibitor, siRNA-BEX2, and miR-370 inhibitor + siRNA-BEX2 groups, with five mice in each group. A xenograft tumor model in nude mice was established under no specific pathogen conditions. The HCC cells at the logarithmic growth phase were collected from each group. After the mice were anaesthetized by aether, HCC cells were inoculated under the skin of the right scapular of them, and subcutaneous uplift was observed when the tumor grew ~4 mm in diameter. The tumor growth condition was observed once every 7 day, and the length and width of the tumor were recorded in detail, with the tumor volume calculated as = (length × width)^2/2. Later on the 35th day, the nude mice were euthanized for extraction of tumors.

Immunohistochemistry

The tissue slices were baked at 60 °C in an oven for 1 h, dewaxed with xylene, hydrated with gradient ethanol, incubated with PBS containing 0.5% Triton at room temperature for 20 min. After being repaired with high-pressure antigen for 2 min, the slices were boiled at 95 °C for 20 min in 0.01 M citric acid buffer (pH 6.0) and sealed with 3% bovine serum albumin blocking solution. Afterwards, the slices were added with the following diluted primary antibodies: rabbit anti-human Bex2 (sc-376342, dilution ratio of 1:200, Santa Cruz Biotechnology, Inc., Santa Cruz, CA, USA) and incubated at 37 °C for 2 h. After that, the HRP-labeled secondary antibody goat anti-rabbit IgG (ab6721, dilution ratio of 1:1000, Abcam Inc., Cambridge, UK) was added for incubation in a 37 °C humidity chamber for 30 min. Thereafter, the slices were counterstained with hematoxylin (Shanghai Fusheng Industrial Co., Ltd, Shanghai, China) at room temperature for 4 min. After being sealed using 10% glycerol/PBS, the slices were observed under a microscope. The results were scored by two persons in an independent manner. The experiment was repeated three times to obtain the mean value.

Statistical analysis

Statistical analyses were processed using the SPSS 21.0 statistical software (IBM Corp. Armonk, NY, USA). Measurement data were expressed as mean ± standard deviation. Comparisons between two groups were carried out by *t*-test, and comparisons among multiple groups were analyzed using one-way analysis of variance (ANOVA). A value of $p < 0.05$ indicated statistical significance.

Results

BEX2 and miR-370 are involved in the development of HCC

The GEO database was applied to search for HCC-related expression data and differential analysis was performed on the obtained expression datasets. The GSE62232 dataset comprised of 286 differentially expressed genes were obtained from the sample patients at young age and 954 from the sample patients at elder age. Simultaneously, 1100 differentially expressed genes were obtained from the GSE62232 dataset by differential analysis. In addition, 30 genes with significantly differential expression were analyzed from the three groups of genes, and a heat map was plotted (Fig. 1a–c). After Venn analysis was performed to obtain the intersection of the top 30 genes with significantly differential expression in the three HCC datasets (Fig. 1d), it was revealed that among the three dataset, six genes overlapped in the analysis results of all the three datasets. Then, the MalaCards database was employed to search for known HCC-associated genes and the top ten genes with the highest score were selected for subsequent analysis (Table 2). In order to further screen the HCC-related genes, further analysis was carried out to probe into the relationship between the ten known genes in the database and the six genes obtained from the three chips, and then a gene interaction network map was constructed (Fig. 1e). The results demonstrated that among these differentially expressed genes, the BEX2 gene interacted with TP53, and TP53 was at the core of the entire interaction network. Therefore, BEX2 expression in the TCGA HCC database was further analyzed, which revealed that the BEX2 gene expression was significantly upregulated in HCC (Fig. 1f). Moreover, former reports have shown that BEX2 can potentially regulate the JNK signaling pathway to promote tumor development [10, 14, 15]. While in HCC, whether the development of HCC was regulated by BEX2 gene through the MAPK/JNK signaling pathway remained to be unclear. Subsequently, to further understand the regulatory mechanism of BEX2 in HCC, the upstream regulating miRNAs of BEX2 were predicted. The regulating miRNAs of BEX2 were predicted in four databases such as DIANA and miRDB, and the prediction results in the four databases were analyzed to find the intersection (Fig. 1g). It was found that there was only one intersected miRNA, the miRNA-hsa-miR-370, regulating the expression of BEX2. These results and existing records indicate that miR-370 can affect the MAPK/JNK signaling pathway through BEX2, thereby regulating the development of HCC.

MiR-370 is poorly expressed while BEX2, JNK, ERK, c-Jun, and c-Fos are highly expressed in HCC tissues

Next, the expression of miR-370, BEX2, JNK, ERK, c-Jun, and c-Fos was detected in HCC and adjacent normal tissues. According to the results of RT-qPCR, compared with the adjacent normal tissues, miR-370 was found to be poorly expressed, while BEX2, JNK, ERK, c-Jun, and c-Fos were highly expressed in HCC tissues (Fig. 2a, b). The findings of western blot analysis revealed that the protein expression of BEX2, JNK, ERK, c-Jun, and c-Fos, as well as the extent of JNK, ERK, and c-Jun phosphorylation was elevated in HCC tissues in comparison with adjacent normal tissues ($p < 0.05$) (Fig. 2c, d).

Expression levels of miR-370 and BEX2 are related with tumor size, vascular invasion, capsular invasion, and TNM staging in patients with HCC

Next, in order to elucidate the relationship between the expressions of miR-370 and BEX2 and the

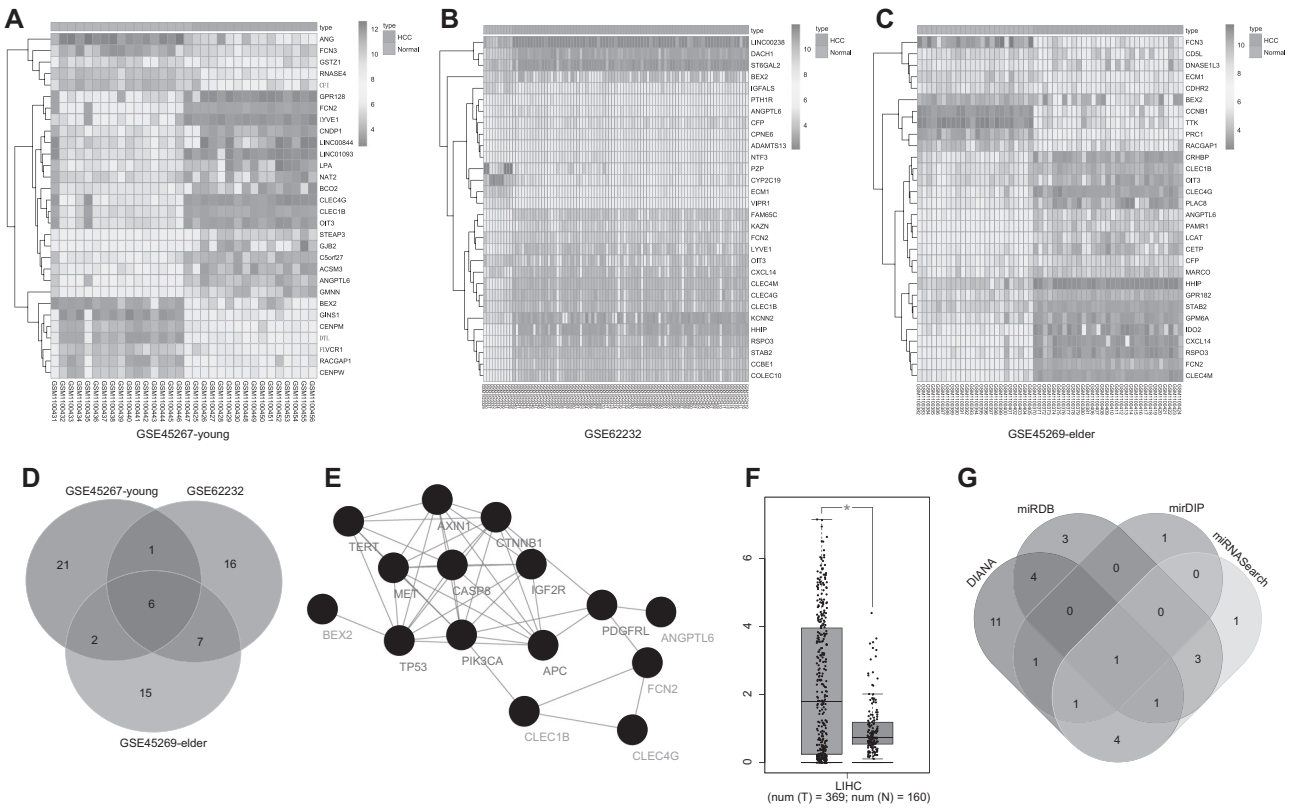

Fig. 1 BEX2 and miR-370 are implicated in the development of HCC. **a**–**c** A heat map of the 30 most differentially expressed genes in three HCC datasets, the abscissa represents the sample number, the ordinate represents the gene name, the upper color bar represents the sample type, the left dendrogram represents clustering analysis of the gene expression, and each block in the graph indicates the expression of a gene in one sample, the square histogram in the upper right shows color gradation. **d** Venn analysis of differentially expressed genes, blue indicates 30 differentially expressed genes obtained from analysis of young samples in the GSE45267 dataset, red indicates 30 differentially expressed genes obtained from GSE62232 dataset, and green indicates 30 differentially expressed genes obtained from middle-aged samples analysis of GSE45267 dataset, the middle part represents the intersected data of the three HCC datasets. **e** Gene interaction network analysis, each ball in the figure represents a gene. Red scripts represent the known genes of HCC obtained by database searching. Green scripts represent differentially expressed genes of HCC obtained by dataset analysis. The connected lines between genes indicate that there is a direct or introductory interaction between any two genes. **f** The expression of BEX2 gene in TCGA HCC database. The red box diagram in the left represents the tumor sample and the gray box diagram in the right represents the normal control sample. **g** Prediction of miRNA which can regulate BEX2, different colors in the image represent the results of miRNA predicted from different databases, and the middle part represents the intersected prediction results of the four database; microRNA-370; BEX2 brain-expressed X-linked protein 2, HCC hepatocellular carcinoma

Table 2 Known genes of HCC

Symbol	Description	Score	PubMed Ids
MET	MET proto-oncogene, receptor tyrosine kinase	1381.34	8276372, 7927256, 8778194
AXIN1	Axin 1	1376.21	10700176, 11526492, 18592156
PIK3CA	Phosphatidylinositol-4,5-bisphosphate 3-kinase catalytic subunit alpha	1358.01	15608678, 15016963, 15520168
IGF2R	Insulin like growth factor 2 receptor	1033.06	9722161, 1337723, 7639583
APC	APC, WNT signaling pathway regulator	1032.92	11466687, 1423316, 10692769
CASP8	Caspase 8	1026.54	15531912, 20403046, 17922191
PDGFRL	Platelet derived growth factor receptor like	1008.5	7898930
CTNNB1	Catenin beta 1	678.61	19728763,17908501, 16094707
TP53	Tumor protein P53	665.13	12800224, 7689531, 12772781
TERT	Telomerase reverse transcriptase	438.57	19627485, 18753050, 11944954

Symbol, abbreviations of the gene names; Description, the gene description or gene full name; Score, this score originates from Solr-based Gene Cards search engine score, obtained by querying the disease in Gene Cards. PubMed Ids, the disease-related reference PMID number for this gene

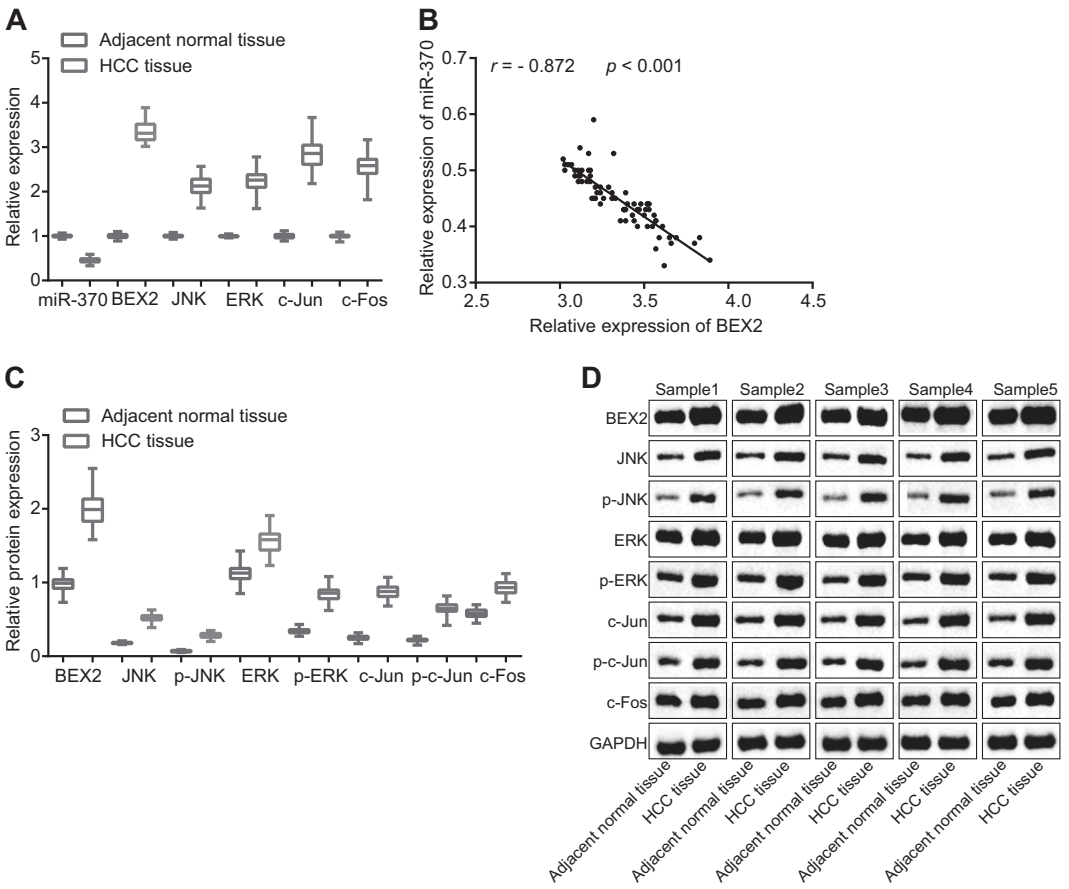

Fig. 2 HCC tissues display decreased miR-370 expression and increased expression of BEX2, JNK, ERK, c-Jun, and c-Fos. **a** miR-370 expression and mRNA expression of BEX2, JNK, ERK, c-Jun, and c-Fos in HCC tissues detected using RT-qPCR. **b** Correlation analysis of BEX2 and miR-370 expression. **c**, **d** Western blot analysis of BEX2, JNK, ERK, c-Jun, and c-Fos proteins as well as extent of JNK, ERK, and c-Jun phosphorylation in adjacent normal tissues and HCC tissues; $^*p < 0.05$ compared with the adjacent normal tissues; $n = 76$, the statistical values in the figure were measurement data, and analyzed by *t*-test; miR-370 microRNA-370, BEX2 brain-expressed X-linked protein 2, JNK Jun NH2 terminal kinase, ERK extracellular-signal-regulated kinases, GAPDH glyceraldehyde-3-phosphate dehydrogenase, HCC hepatocellular carcinoma

clinicopathological features of patients with HCC, Table 3 is listed. According to the table, the expression of miR-370 and BEX2 was not related to age, gender, and the occurrence of cirrhosis ($p > 0.05$), while exhibiting association with tumor size, vascular invasion, capsule invasion, and TNM staging in patients with HCC ($p < 0.05$).

Hep3B cell line with the highest BEX2 expression and the lowest miR-370 expression is selected as the study subject

In addition, RT-qPCR and western blot analysis were applied to detect the miR-370 expression and the mRNA and protein expression of BEX2 in the six HCC cell lines (Hep3B, SK-hep-1, YY8103, MHCC-97H, C3A, HepG2). The mRNA and protein expression of BEX2 was found to be similar (Fig. 3a–c). Hep3B cell line exhibiting highest BEX2 expression and the lowest miR-370 expression was selected for further experimentation.

Overexpressed miR-370 inhibits BEX2, a target gene of miR-370 and disrupts activation of the MAPK/JNK signaling pathway

Online software analysis results (Fig. 4a) indicated the presence of a specific binding site between the BEX2 gene sequence and the miR-370 sequence. Dual luciferase reporter gene assay data verified that BEX2 was a target gene of miR-370 (Fig. 4b). The luciferase activity of BEX2-Wt co-transfected with miR-370 was found to be decreased compared with the NC group ($p < 0.05$), while that of the BEX2-Mut co-transfected with miR-370 remained unaffected ($p > 0.05$). These findings indicated that miR-370 can specifically bind to the BEX2 gene, and BEX2 is a target gene of miR-370.

Table 3 Relative expression of miR-370 and BEX2 correlates with tumor size, vascular invasion, capsular invasion, and TNM staging in patients with HCC

Clinicopathological data	Number of cases	Relative expression of miR-370	*p* value	Relative expression of BEX2	*p* value
Age (year)					
<55	36	0.46 ± 0.04	0.342	3.32 ± 0.20	0.411
≥55	40	0.45 ± 0.05		3.36 ± 0.22	
Gender					
Male	42	0.46 ± 0.05	0.087	3.30 ± 0.20	0.06
Female	34	0.44 ± 0.05		3.39 ± 0.21	
Liver cirrhosis					
Yes	44	0.44 ± 0.04	0.057	3.37 ± 0.23	0.157
No	32	0.46 ± 0.05		3.30 ± 0.18	
Tumor size(cm)					
<5	17	0.48 ± 0.05	0.005	3.18 ± 0.17	<0.001
≥5	59	0.44 ± 0.05		3.39 ± 0.20	
Vascular invasion					
Yes	37	0.42 ± 0.04	<0.001	3.48 ± 0.15	<0.001
No	39	0.48 ± 0.04		3.21 ± 0.17	
TNM staging					
I/II stage	48	0.48 ± 0.04	<0.001	3.21 ± 0.12	<0.001
III/IV stage	28	0.41 ± 0.03		3.56 ± 0.15	
Encroachment					
Yes	40	0.42 ± 0.03	<0.001	3.49 ± 0.16	<0.001
No	36	0.49 ± 0.03		3.17 ± 0.10	

BEX2 brain-expressed X-linked protein 2, *miR*-370 microRNA-370, *TNM* tumor node metastasis

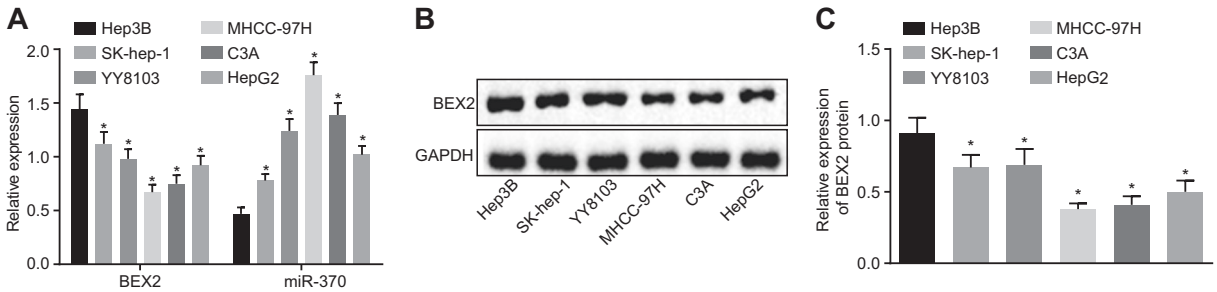

Fig. 3 Hep3B cell line presents with the highest BEX2 expression and the lowest miR-370 expression. **a** miR-370 expression and mRNA expression of BEX2 in HCC cell lines detected using RT-qPCR. **b**, **c** Western blot analysis of BEX2 protein in HCC cell lines; *$p < 0.05$ compared with Hep3B cell line; the statistical values in the figure were measurement data, and analyzed by one-way ANOVA; the experiment was repeated three times; BEX2 brain-expressed X-linked protein 2, miR-370 microRNA-370, HCC hepatocellular carcinoma

Then, the expression of miR-370, BEX2, JNK, ERK, c-Jun, and c-Fos in different transfection groups was assessed using RT-qPCR and western blot analysis. As shown in Fig. 4c–e, there was no significant difference in the expression of the above factors between the blank and NC groups ($p > 0.05$). Compared with the blank group, miR-370 expression was noted to be significantly increased in the miR-370 mimic group ($p < 0.05$), which was significantly decreased in the miR-370 inhibitor and miR-370 inhibitor + siRNA-BEX2 groups ($p < 0.05$); however, no evident difference was observed in the siRNA-BEX2 group ($p > 0.05$). Compared with the blank group, the mRNA and protein expression of BEX2, JNK, ERK, c-Jun, and c-Fos was significantly decreased in the miR-370 mimic and siRNA-BEX2 groups ($p < 0.05$), while was elevated in the miR-370 inhibitor group ($p < 0.05$); also, they were not significantly different in the miR-370 inhibitor + siRNA-BEX2 group ($p > 0.05$). Compared with the blank group, the extent of JNK, ERK, and c-Jun phosphorylation was decreased in the miR-370 mimic and siRNA-BEX2 groups ($p < 0.05$), whereas increased findings were observed in the miR-370 inhibitor group ($p < 0.05$); however, the miR-370 inhibitor + siRNA-BEX2 group showed no statistical changes ($p > 0.05$).

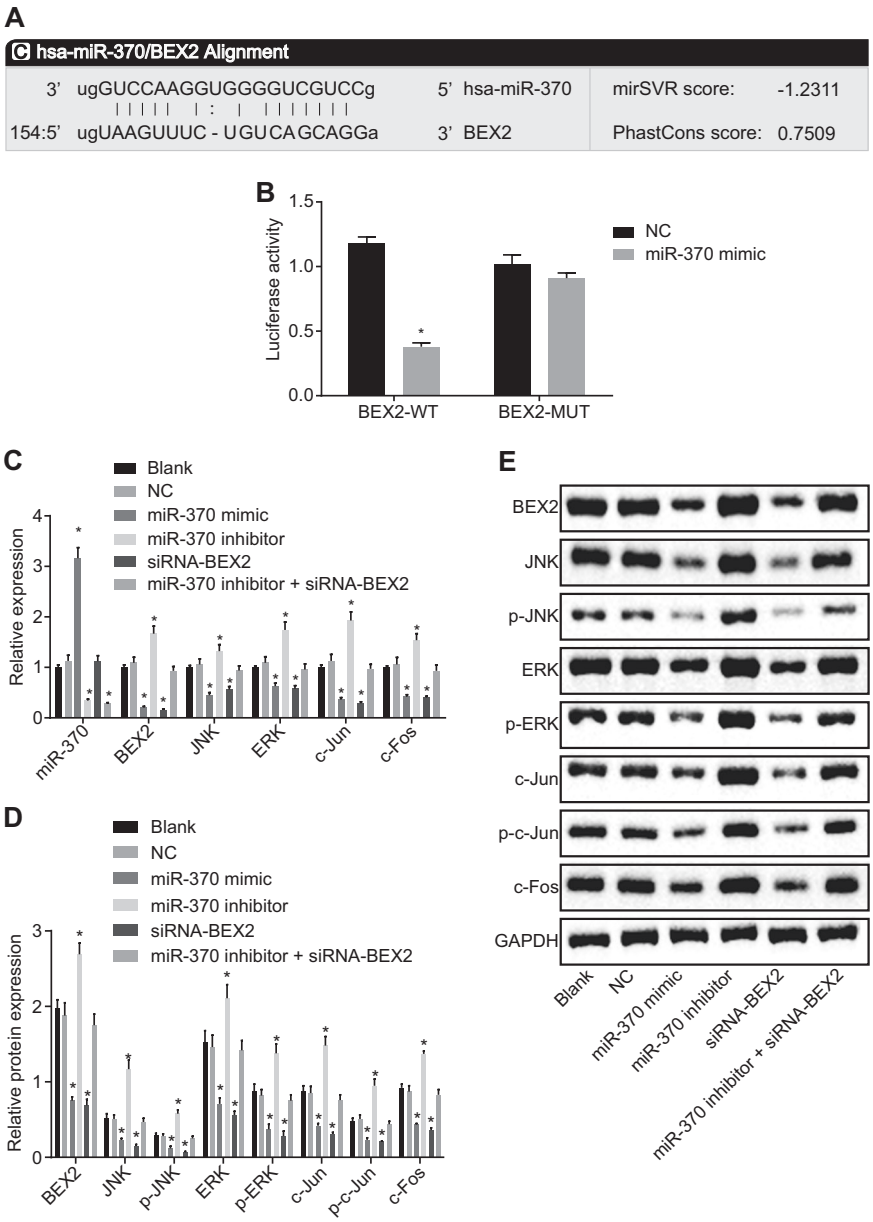

Fig. 4 BEX2 is a target gene of miR-370 and overexpressed miR-370 inhibits BEX2 and activation of MAPK/JNK signaling pathway. **a** The predicted binding site of miR-370 and BEX2. **b** The luciferase activity of the BEX2-Wt and BEX2-Mut detected using dual luciferase reporter gene assay; $*p < 0.05$ compared with the NC group. **c** miR-370 expression and mRNA expression of BEX2, JNK, ERK, c-Jun, and c-Fos detected using RT-qPCR; D and E, western blot analysis of BEX2, JNK, ERK, c-Jun, and c-Fos proteins and the extent of JNK, ERK, and c-Jun phosphorylation; $*p < 0.05$ compared with the blank group; the statistical values in the figure were measurement data, and were analyzed by *t*-test; the experiment was repeated three times; BEX2 brain-expressed X-linked protein 2, miR-370 microRNA-370, NC negative control

miR-370 overexpression and BEX2 silencing inhibit HCC cell proliferation and promote apoptosis

MTT assay was further applied to detect the proliferation of HCC cells after different transfection. The MTT results (Fig. 5a) revealed that there was no significant difference in cell proliferation among the six groups at 24 h after the transfection ($p > 0.05$). After transfection for 24 h, there was no significantly difference in cell proliferation between the blank and NC groups ($p > 0.05$). Compared with the blank group, the HCC cell proliferation in the miR-370 mimic and siRNA-BEX2 groups was decreased ($p < 0.05$), while opposite trends were noted in the miR-370 inhibitor group ($p < 0.05$) and was not significantly different in the miR-370 inhibitor + siRNA-BEX2 group ($p > 0.05$). The results showed that overexpression of miR-370 and BEX2 silencing could inhibit the proliferation of HCC cells.

In addition, HCC cell cycle and cell apoptosis were detected by means of flow cytometry. Figure 5b, c showed that there was no significant difference of cell apoptosis between the blank group and the NC group ($p > 0.05$). Compared with the blank group, the miR-370 inhibitor group exhibited less G1 phase-arrested cells and more S phase-arrested cells ($p < 0.05$), while the miR-370 mimic and siRNA-BEX2 groups demonstrated opposite trends. There was no significant difference in the cell cycle between the blank and miR-370 inhibitor + siRNA-BEX2 groups ($p > 0.05$).

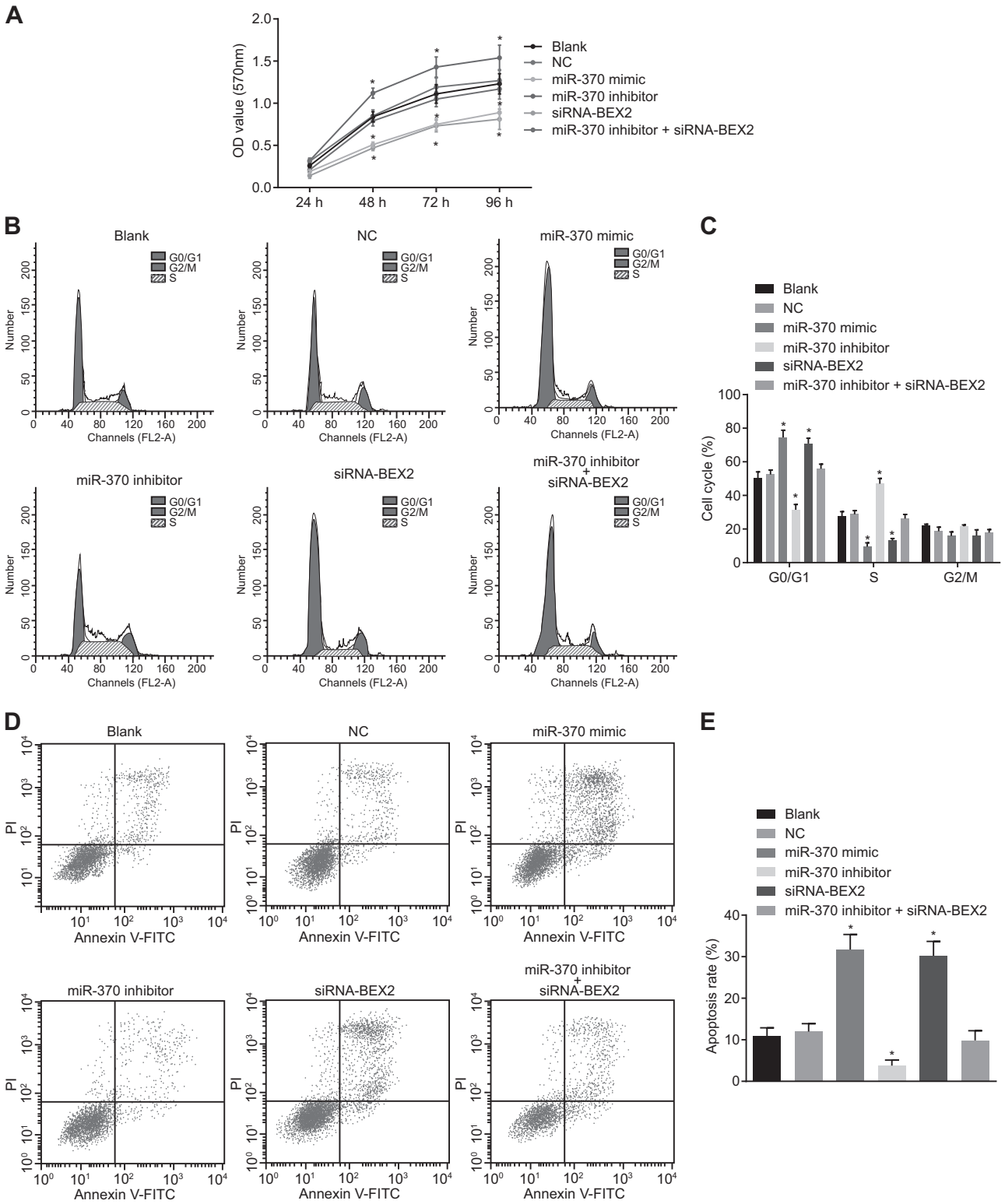

Fig. 5 HCC cell proliferation is suppressed while apoptosis is induced after transfection with miR-370 overexpression and BEX2 down-regulation. **a** Cell proliferation after transfection measured using MTT assay. **b** HCC cell cycle after transfection. **c** The proportion of cells arrested in different phase after transfection. **d**, **e** HCC cell apoptosis after transfection measured using flow cytometry; *$p < 0.05$ compared with the blank group, the statistical values in the figure were measurement data and analyzed using repeated measurement ANOVA. The experiment was repeated three times; miR-370 microRNA-370, BEX2 brain-expressed X-linked protein 2, HCC hepatocellular carcinoma

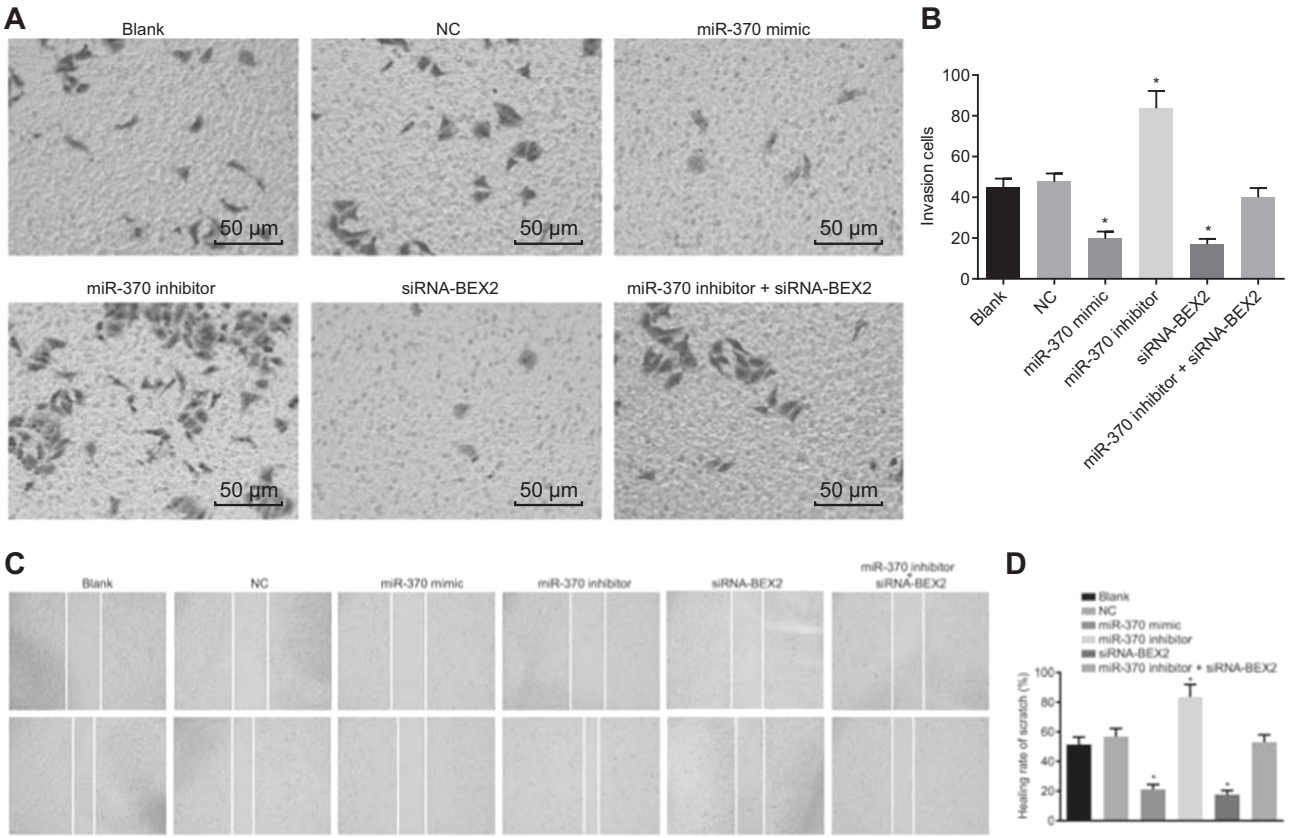

Fig. 6 HCC cell migration and invasion are inhibited by miR-370 overexpression or BEX2 silencing. **a** Cell invasion after transfection observed under an inverted microscope. **b** The statistical results of the invasion experiment. **c** The migration of cells at 0 and 24 h after transfection measured using Scratch test. **d** The healing rate of scratches in each group after transfection. *$p < 0.05$ compared with blank group, the statistical values in the figure were measurement data and analyzed using one-way ANOVA; the experiment was repeated three times; miR-370 microRNA-370, HCC hepatocellular carcinoma

The results of cell apoptosis (Fig. 5d, e) revealed no significant difference in cell apoptosis between the blank group and the NC group ($p > 0.05$). Compared with the blank group, HCC cell apoptosis was significantly decreased in the miR-370 inhibitor group ($p < 0.05$), while was promoted in the miR-370 mimic and siRNA-BEX2 groups ($p < 0.05$). There was no significant difference in the apoptosis rate of HCC cells in the miR-370 inhibitor + siRNA-BEX2 group when compared with the blank group ($p > 0.05$).

The aforementioned results showed that overexpression of miR-370 and BEX2 silencing could accelerate HCC cell proliferation and decelerate cell apoptosis.

miR-370 overexpression and BEX2 silencing impede HCC cell migration and invasion

The transwell assay was performed to analyze the cell invasion in each group after transfection, and results showed (Fig. 6a, b) no significant difference in the number of invasive cells in the blank group and the NC group ($p > 0.05$). Compared with the blank group, miR-370 inhibitor group showed significantly increased number of invasive cells and enhanced invasive ability; the miR-370 mimic and siRNA-BEX2 groups presented with significantly decreased number of invasive cells and diminished invasive ability (both $p < 0.05$), while there was no significant difference in invasive ability in miR-370 inhibitor + siRNA-BEX2 group ($p > 0.05$). The results showed that overexpression of miR-370 could inhibit HCC cell invasion.

Scratch test was further conducted to analyze the migration of HCC cells in different transfection groups. As shown in Fig. 6c, d, the scratches of cells in each group were observed after transfection at 0 and 24 h, respectively. There was no significant difference in the healing rate of HCC cells at 0 h in each group ($p > 0.05$). Also, there was no significant difference in relation to migration ability between the blank and NC groups ($p > 0.05$). Compared with the blank group, the healing rate of cells after scratch was significantly increased in the miR-370 inhibitor group, and the migration ability was significantly raised ($p < 0.05$). Compared with the blank group, the cells in the miR-370 mimic and siRNA-BEX2 groups presented with decreased healing rate and declined

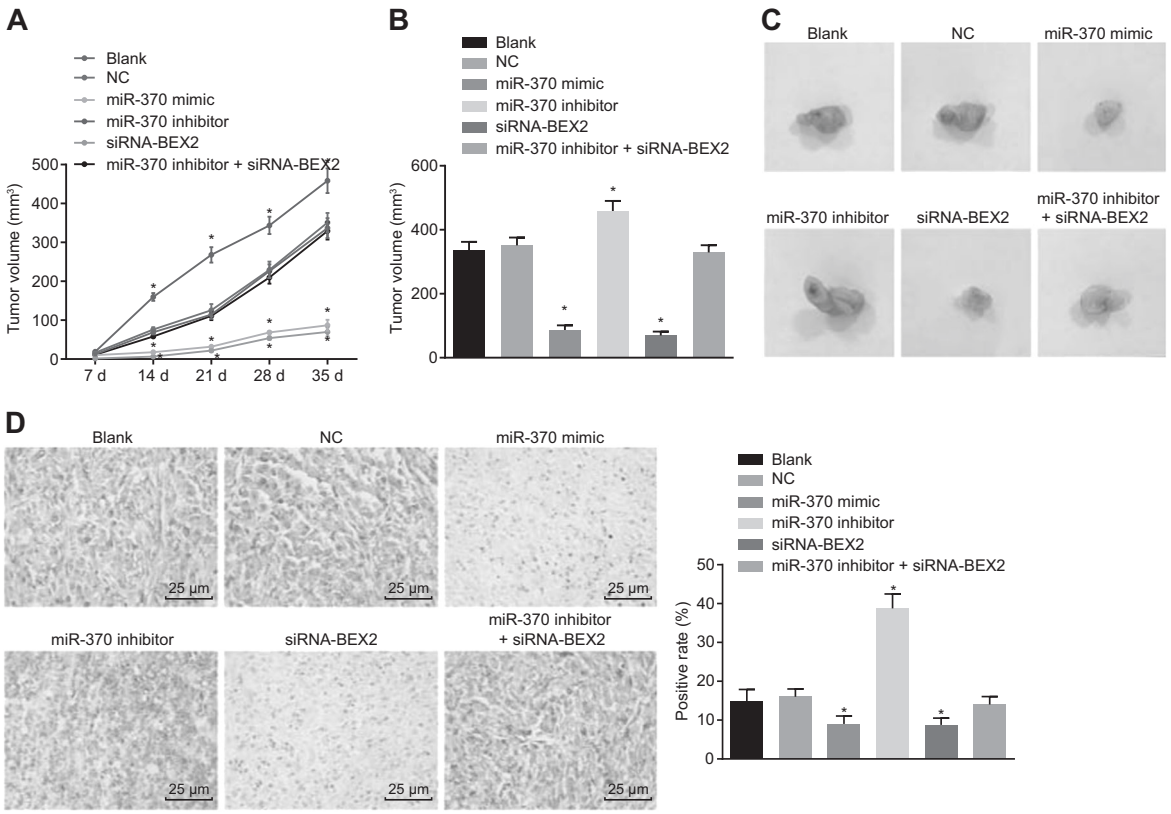

Fig. 7 Smaller tumor size and decreased tumor growth rate are observed in mice injected with siRNA-BEX2 and miR-370 mimic. **a** Line chart of the growth of tumor volume after transfection. **b** The diagram of tumor volume on the 35th day after transfection. **c** Tumor size and volume after transfection on the 35th day **d** Immunohistochemistry analysis of BEX protein; $^*p < 0.05$ compared with the blank group; $n = 5$; the statistical values in the figure were measurement data and analyzed by one-way ANOVA and repeated measurement ANOVA; miR-370 microRNA-370, BEX2 brain-expressed X-linked protein 2, HCC hepatocellular carcinoma

migration ability ($p < 0.05$), and no significant difference was observed in the miR-370 inhibitor + siRNA-BEX2 group ($p > 0.05$).

Altogether, the results showed that overexpression of miR-370 and BEX2 silencing could potentially inhibit the migration and invasion of HCC cells.

miR-370 overexpression slows down HCC tumor growth

At last, tumor size was measured in each group after different transfection. The results in Fig. 7a–c showed there was no significant difference in tumor size between the blank and NC groups ($p > 0.05$). Compared with the blank group, there was no significant difference in tumor size in the miR-370 inhibitor + siRNA-BEX2 group ($p > 0.05$). After 14 days of transfection, the subcutaneous tumor of mice was found to be significantly larger, and the tumor growth rate was the fastest in the miR-370 inhibitor group relative to the blank group ($p < 0.05$); while, the growth rate and size of subcutaneous tumor in mice were significantly slower and smaller in the miR-370 mimic and siRNA-BEX2 groups than those in the blank group ($p < 0.05$). On the 35th day, the expression of BEX2 was quantified using immunohistochemistry (Fig. 7d). The results showed that there was no significant difference in relation to the positive expression of BEX2 protein between the blank group and the NC group ($p > 0.05$). Compared with the blank group, the positive expression of BEX2 protein showed no significant difference in the miR-370 inhibitor + siRNA-BEX2 group ($p > 0.05$). The positive expression of BEX2 protein was found to be significantly increased in the miR-370 inhibitor group, while that of BEX2 was significantly decreased in the miR-370 mimic group and the siRNA-BEX2 group when compared with the blank group.

Taken together, miR-370 could downregulate BEX2 and inhibit tumor growth in mice with HCC.

Discussion

HCC has appeared to be a major cause resulting in cancer-related deaths, ranking as an urgent priority on the agenda of medical treatment [16]. MiRNAs are consisted of a group of small noncoding RNAs who function to mediate a great

deal of cellular physiological activities, including cell development, proliferation, differentiation, and apoptosis, by regulating the target genes at a posttranscriptional level [17]. BEX2 is a member of the BEX gene family, which influences the nervous system and neurological diseases [18]. The current study aimed to investigate the effects of miR-370 on cell cycle, proliferation, invasion, migration, and apoptosis of HCC cells by mediating the MARK/JNK signaling pathway through regulation of BEX2. The findings of this study supported the conclusion that miR-370 overexpression could potentially inhibit the activation of the MAPK/JNK signaling pathway by negatively targeting BEX2, thereby preventing the initiation and progression of HCC.

Firstly, we uncovered that miR-370 was expressed lowly and BEX2 was expressed at high levels in HCC tissues. A previous study showed that the downregulation of miR-370 resulted in promoted tumor cell proliferation, cell cycle procession, and tumor colony formation in gastric cancer [19]. It was also revealed by former researchers that miR-370 upregulation leads to promoted apoptosis and suppressed proliferation in nonsmall cell lung cancer tissues and cell lines [20]. In addition, a recent study reported that miR-370 was poorly expressed in colon cancer tissues compared with adjacent normal tissues, which is similar to our findings of low miR-370 in HCC tissues [7]. Furthermore, BEX2 is highly expressed in a subset of estrogen receptor-positive breast cancers and glioblastoma, and also plays a vital role in promoting tumor cell survival and growth in breast cancer [21, 22]. Thus, it can be verified that miR-370 may play an important role in the development of HCC. It has further been reported that miRNA profiling can be regulated by both epigenetic modifications change and late-onset hypogonadism (LOH). Previous studies have also shown that LOH is associated with a plasma miRNA expression profile that was different from normal [23]. Moreover, miR-212 has also been demonstrated to be downregulated in human CRC tissues via genetic and epigenetic mechanisms [24]. These findings could help figure out the upstream regulatory mechanism of miR-370 profiling during HCC development. Furthermore, we confirmed that BEX2 was a target of miR-370 by bioinformatics prediction and dual luciferase reporter gene assay. More importantly, our findings revealed that overexpression of miR-370 downregulated BEX2 gene, inhibited the activation of the MAPK/JNK signaling pathway by downregulating the pathway-related genes. According to a former study, CASZ1 suppresses HCC growth by inhibiting the MAPK/ERK signaling pathway [25]. Naderi et al. further reported that downregulation of BEX2 could decrease the extent of c-Jun phosphorylation and diminish the migration ability of breast cancer cells, which would make a massive difference in the treatment of HCC [15]. Also, the relatively overexpressed BEX2 in breast tumors could be explained as an effect of highly regulated c-Jun factor in the mechanism of breast cancer [15]. C-Fos was also confirmed to serve as a significant physiological marker for neural activation [26]. The repression of matrix metalloproteinase-1 by c-Fos inhibition has also been previously demonstrated to suppress HCC cell migration and invasion [27]. In consistent with the above findings, the expression of MARK/JNK signaling pathway-related genes was downregulated after treatment of BEX2 inhibition and miR-370 overexpression. Therefore, miR-370 could benefit HCC treatment by negatively regulating BEX2 and inactivating the MARK/JNK signaling pathway.

Also, the findings in the current study proved that miR-370 mimic and BEX2 silencing inhibited proliferation, migration, invasion, while promoted apoptosis of HCC cells. Overexpression of miR-370 has previously been revealed to suppress cell migration and invasion of HCC cells by inhibition of the oncoprotein LIN28A [28]. Also, the overexpression of miR-370 speeds up the apoptosis of HCC cell lines [29]. BEX2 downregulation is known to promote cell apoptosis in malignant glioma cells and activate the JNK signaling pathway [10]. What is more, BEX2 plays an important role in promoting cell survival and growth in breast cancer cells [15]. The above findings were in consistent with those obtained from our study that miR-370 overexpression promoted apoptosis and inhibited proliferation, migration, invasion of HCC cells. Furthermore, in vivo experiment results in our study demonstrated that overexpression of miR-370 inhibited tumor size and tumor growth, which also confirmed the above conclusions.

In conclusion, the current study evidenced decreased miR-370 expression and increased BEX2 expression in HCC cells and tissues. A negative correlation between miR-370 in BEX2 was also proved. In addition, miR-370 overexpression can promote apoptosis and inhibit proliferation, migration and invasion of HCC cells through suppression of the MAPK/JNK signaling pathway by downregulating BEX2 (Fig. 8). These findings may open novel avenues for future HCC therapies. However, since HCC under different background, such as HBV, HVC, or no virus infection, may have some reverse regulatory effects on the expression of miR-370, therefore, further studies are warranted to explore the specific mechanism of miR-370 in HCC.

Acknowledgements We would also like to thank all participants enrolled in the present study.

Funding This study was supported by the Hubei Chen Xiaoping Science and Technology Development Foundation—Henrui Research Foundation of Malignant Tumors of Liver, Gallbladder and Pancreas

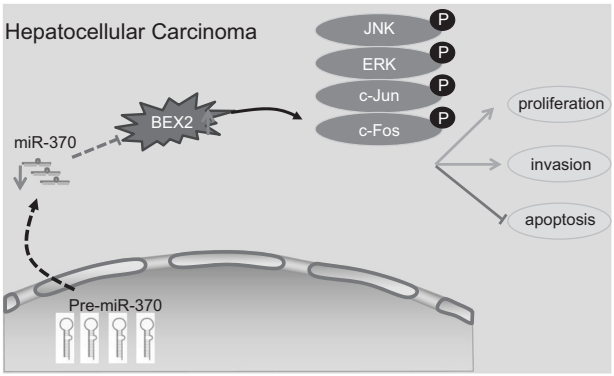

Fig. 8 miR-370 regulates the MAPK/JNK signaling pathway via BEX2, thus to influence the progression of HCC. In HCC, the expression of miR-370 was significantly downregulated, which in turn led to the upregulation of BEX2 gene expression. Elevated miR-370 expression functions to promote the proliferation and invasion, while inhibit the apoptosis of HCC through inhibition of the MAPK/JNK signaling pathway by downregulating BEX2. p in the figure represents phosphorylation

(CXPJJH11800001–2018320), Medical and Health Science and Technology Development Plan Project of Shandong Province (2016WS0272), and Project "Clinical Medicine + X" of Medical Department of Qingdao University.

Compliance with ethical standards

Conflict of interest The authors declare that they have no conflict of interest.

Ethics statement All experimental procedures were approved by the Ethics Committee, as well as the Animal Care and Use Committee of the Affiliated Hospital of Qingdao University. Signed informed consents were obtained from all patients, or their parents and guardians. All efforts were made to minimize the suffering of the included animals.

Publisher's note Springer Nature remains neutral with regard to jurisdictional claims in published maps and institutional affiliations.

References

1. Siegel RL, Miller KD, Jemal A. Cancer statistics, 2015. Cancer J Clin. 2015;65:5–29.
2. Lv J, Kong Y, Gao Z, Liu Y, Zhu P, Yu Z. LncRNA TUG1 interacting with miR-144 contributes to proliferation, migration and tumorigenesis through activating the JAK2/STAT3 pathway in hepatocellular carcinoma. Int J Biochem Cell Biol. 2018;101:19–28.
3. Zhang J, Zhang D, Zhao Q, Qi J, Li X, Qin C. A distinctively expressed long noncoding RNA, RP11-466I1.1, may serve as a prognostic biomarker in hepatocellular carcinoma. Cancer Med. 2018. https://doi.org/10.1002/cam4.1565
4. Wiemer EA. The role of microRNAs in cancer: no small matter. Eur J Cancer. 2007;43:1529–44.
5. Han G, Zhang L, Ni X, Chen Z, Pan X, Zhu Q, et al. MicroRNA-873 promotes cell proliferation, migration, and invasion by directly targeting TSLC1 in hepatocellular carcinoma. Cell Physiol Biochem. 2018;46:2261–70.
6. Lv J, Xia K, Xu P, Sun E, Ma J, Gao S, et al. miRNA expression patterns in chemoresistant breast cancer tissues. Biomed Pharmacother. 2014;68:935–42.
7. Shen X, Zuo X, Zhang W, Bai Y, Qin X, Hou N. MiR-370 promotes apoptosis in colon cancer by directly targeting MDM4. Oncol Lett. 2018;15:1673–9.
8. Lu M, Wang Y, Zhou S, Xu J, Li J, Tao R, et al. MicroRNA-370 suppresses the progression and proliferation of human astrocytoma and glioblastoma by negatively regulating beta-catenin and causing activation of FOXO3a. Exp Ther Med. 2018;15:1093–8.
9. Huang F, Cai P, Wang Y, Zhou X, Chen H, Liao W, et al. Up-regulation of brain-expressed X-linked 2 is critical for hepatitis B virus X protein-induced hepatocellular carcinoma development. Oncotarget. 2017;8:65789–99.
10. Zhou X, Meng Q, Xu X, Zhi T, Shi Q, Wang Y, et al. Bex2 regulates cell proliferation and apoptosis in malignant glioma cells via the c-Jun NH2-terminal kinase pathway. Biochem Biophys Res Commun. 2012;427:574–80.
11. Papa S, Bubici C. Feeding the Hedgehog: a new meaning for JNK signalling in liver regeneration. J Hepatol. 2018;69:572–4.
12. Chen Z, Zuo X, Zhang Y, Han G, Zhang L, Wu J, et al. MiR-3662 suppresses hepatocellular carcinoma growth through inhibition of HIF-1alpha-mediated Warburg effect. Cell Death Dis. 2018;9:549.
13. Leung TW, Tang AM, Zee B, Lau WY, Lai PB, Leung KL, et al. Construction of the Chinese University Prognostic Index for hepatocellular carcinoma and comparison with the TNM staging system, the Okuda staging system, and the Cancer of the Liver Italian Program staging system: a study based on 926 patients. Cancer 2002;94:1760–9.
14. Hu Y, Xiao Q, Chen H, He J, Tan Y, Liu Y, et al. BEX2 promotes tumor proliferation in colorectal cancer. Int J Biol Sci. 2017;13:286–94.
15. Naderi A, Liu J, Hughes-Davies L. BEX2 has a functional interplay with c-Jun/JNK and p65/RelA in breast cancer. Mol Cancer. 2010;9:111.
16. Yu LX, Ling Y, Wang HY. Role of nonresolving inflammation in hepatocellular carcinoma development and progression. NPJ Precis Oncol 2018;2:6.
17. Pan XP, Wang HX, Tong DM, Li Y, Huang LH, Wang C. miRNA-370 acts as a tumor suppressor via the downregulation of PIM1 in hepatocellular carcinoma. Eur Rev Med Pharmacol Sci. 2017;21:1254–63.
18. Zhou X, Xu X, Meng Q, Hu J, Zhi T, Shi Q, et al. Bex2 is critical for migration and invasion in malignant glioma cells. J Mol Neurosci. 2013;50:78–87.
19. Zeng Y, Fu M, Wu GW, Zhang AZ, Chen JP, Lin HY, et al. Upregulation of microRNA-370 promotes cell apoptosis and inhibits proliferation by targeting PTEN in human gastric cancer. Int J Oncol. 2016;49:1589–99.
20. Chen T, Gao F, Feng S, Yang T, Chen M. MicroRNA-370 inhibits the progression of non-small cell lung cancer by downregulating oncogene TRAF4. Oncol Rep. 2015;34:461–8.
21. Naderi A, Liu J, Bennett IC. BEX2 regulates mitochondrial apoptosis and G1 cell cycle in breast cancer. Int J Cancer. 2010;126:1596–610.
22. Meng Q, Zhi T, Chao Y, Nie E, Xu X, Shi Q, et al. Bex2 controls proliferation of human glioblastoma cells through NF-kappaB signaling pathway. J Mol Neurosci. 2014;53:262–70.
23. Russell N, Grossmann M. Plasma miRNA expression profile in the diagnosis of late-onset hypogonadism. Asian J Androl. 2016;18:713–5.

24. Meng X, Wu J, Pan C, Wang H, Ying X, Zhou Y, et al. Genetic and epigenetic down-regulation of microRNA-212 promotes colorectal tumor metastasis via dysregulation of MnSOD. Gastroenterology. 2013;145:426–36, e1–6.
25. Wang JL, Yang MY, Xiao S, Sun B, Li YM, Yang LY. Down-regulation of castor zinc finger 1 predicts poor prognosis and facilitates hepatocellular carcinoma progression via MAPK/ERK signaling. J Exp Clin Cancer Res. 2018;37:45.
26. Chen Y, Yamaguchi Y, Suzuki T, Doi M, Okamura H. Effect of daily light on c-Fos expression in the suprachiasmatic nucleus under jet lag conditions. Acta Histochem Cytochem. 2018;51:73–80.
27. Fan Q, He M, Deng X, Wu WK, Zhao L, Tang J, et al. Derepression of c-Fos caused by microRNA-139 down-regulation contributes to the metastasis of human hepatocellular carcinoma. Cell Biochem Funct. 2013;31:319–24.
28. Xu WP, Yi M, Li QQ, Zhou WP, Cong WM, Yang Y, et al. Perturbation of MicroRNA-370/Lin-28 homolog A/nuclear factor kappa B regulatory circuit contributes to the development of hepatocellular carcinoma. Hepatology. 2013;58:1977–91.
29. Liu Z, Ma M, Yan L, Chen S, Li S, Yang D, et al. miR-370 regulates ISG15 expression and influences IFN-alpha sensitivity in hepatocellular carcinoma cells. Cancer Biomark. 2018;22:453–66.